

Reaction of Cyclic Nitroxides with Nitrogen Dioxide: The Intermediacy of the Oxoammonium Cations

Sara Goldstein,^{*,†} Amram Samuni,[‡] and Angelo Russo[§]

Contribution from the Department of Physical Chemistry, The Hebrew University of Jerusalem, Jerusalem 91904, Israel, Department of Molecular Biology, Hebrew University-Hadassah Medical School, P.O. Box 12000, Jerusalem 91120, Israel, and Radiation Biology Branch, National Cancer Institute, NIH, Bethesda, Maryland 20892

Received March 23, 2003; E-mail: sarag@vms.huji.ac.il

Abstract: Piperidine and pyrrolidine nitroxides, such as 2,2,6,6-tetramethylpiperidinoxyl (TPO) and 3-carbamoylproxyl (3-CP), respectively, are cell-permeable stable radicals, which effectively protect cells, tissues, isolated organs, and laboratory animals from radical-induced damage. The kinetics and mechanism of their reactions with $\cdot\text{OH}$, superoxide, and carbon-centered radicals have been extensively studied, but not with $\cdot\text{NO}_2$, although the latter is a key intermediate in cellular nitrosative stress. In this research, $\cdot\text{NO}_2$ was generated by pulse radiolysis, and its reactions with TPO, 4-OH-TPO, 4-oxo-TPO, and 3-CP were studied by fast kinetic spectroscopy, either directly or by using ferrocyanide or 2,2'-azino-bis(3-ethylbenzothiazoline-6-sulfonate), which effectively scavenge the product of this reaction, the oxoammonium cation. The rate constants for the reactions of $\cdot\text{NO}_2$ with these nitroxides were determined to be $(7-8) \times 10^8 \text{ M}^{-1} \text{ s}^{-1}$, independent of the pH over the range 3.9–10.2. These are among the highest rate constants measured for $\cdot\text{NO}_2$ and are close to that of the reaction of $\cdot\text{NO}_2$ with $\cdot\text{NO}$, that is, $1.1 \times 10^9 \text{ M}^{-1} \text{ s}^{-1}$. The hydroxylamines TPO-H and 4-OH-TPO-H are less reactive toward $\cdot\text{NO}_2$, and an upper limit for the rate constant for these reactions was estimated to be $1 \times 10^5 \text{ M}^{-1} \text{ s}^{-1}$. The kinetics results demonstrate that the reaction of nitroxides with $\cdot\text{NO}_2$ proceeds via an inner-sphere electron-transfer mechanism to form the respective oxoammonium cation, which is reduced back to the nitroxide through the oxidation of nitrite to $\cdot\text{NO}_2$. Hence, the nitroxide slows down the decomposition of $\cdot\text{NO}_2$ into nitrite and nitrate and could serve as a reservoir of $\cdot\text{NO}_2$ unless the respective oxoammonium is rapidly scavenged by other reductant. This mechanism can contribute toward the protective effect of nitroxides against reactive nitrogen-derived species, although the oxoammonium cations themselves might oxidize essential cellular targets if they are not scavenged by common biological reductants, such as thiols.

Introduction

The increasing knowledge of the roles played by free radical in disease processes has expanded the search for more efficient antioxidants that will diminish radical-induced damage. Cyclic nitroxides, such as 2,2,6,6-tetramethylpiperidinoxyl (TPO), are cell-permeable stable radicals, which effectively protect cells, tissues, isolated organs, and laboratory animals from radical-induced damage.^{1–7} Their protective effects have, in part, been

attributed to their ability to catalyze superoxide dismutation,^{1,8} as well as detoxification of carbon-centered radicals^{9–11} and alkoxy and peroxy radicals.^{12,13} The kinetics and mechanisms of the reactions of nitroxides with nitrogen-derived reactive species are far from being elucidated. It has been shown that $\cdot\text{NO}$ reacts with nitronyl nitroxides^{14–16} and aromatic nitroxides,^{17,18} but there is no agreement on the mechanism of this reaction. Likewise, there is no agreement regarding the reactivity

[†] The Hebrew University of Jerusalem.

[‡] Hebrew University-Hadassah Medical School.

[§] National Cancer Institute.

- (1) Mitchell, J. B.; Samuni, A.; Krishna, M. C.; DeGraff, W. G.; Ahn, M. S.; Samuni, U.; Russo, A. *Biochemistry* **1990**, *29*, 2802–2807.
- (2) Samuni, A.; Godinger, D.; Aronovitch, J.; Russo, A.; Mitchell, J. B. *Biochemistry* **1991**, *30*, 555–561.
- (3) Konovalova, N. P.; Diatchkovskaya, R. F.; Volkova, L. M.; Varfolomeev, V. N. *Anti-Cancer Drugs* **1991**, *2*, 591–595.
- (4) Reddan, J. R.; Sevilla, M. D.; Giblin, F. J.; Padgaonkar, V.; Dziedzic, D. C.; Leverenz, V.; Misra, I. C.; Peters, J. L. *Exp. Eye Res.* **1993**, *56*, 543–554.
- (5) Miura, Y.; Utsumi, H.; Hamada, A. *Arch. Biochem. Biophys.* **1993**, *300*, 148–156.
- (6) Howard, B. J.; Yatin, S.; Hensley, K.; Allen, K. L.; Kelly, J. P.; Carney, J.; Butterfield, D. A. *J. Neurochem.* **1996**, *67*, 2045–2050.
- (7) Chatterjee, P. K.; Cuzzocrea, S.; Brown, P. A. J.; Zacharowski, K.; Stewart, K. N.; Mota-Filipe, H.; Thiemermann, C. *Kidney Int.* **2000**, *58*, 658–673.

- (8) Samuni, A.; Krishna, C. M.; Riesz, P.; Finkelstein, E.; Russo, A. *J. Biol. Chem.* **1988**, *263*, 17921–17924.
- (9) Beckwith, A. L. J.; Bowry, V. W.; Ingold, K. U. *J. Am. Chem. Soc.* **1992**, *114*, 4983–4992.
- (10) Bowry, V. W.; Ingold, K. U. *J. Am. Chem. Soc.* **1992**, *114*, 4992–4996.
- (11) Brede, O.; Beckert, D.; Windolph, C.; Gottinger, H. A. *J. Phys. Chem. A* **1998**, *102*, 1457–1464.
- (12) Nilsson, U. A.; Carlin, G.; Bylundfellenius, A. C. *Chem.-Biol. Interact.* **1990**, *74*, 325–342.
- (13) Offer, T.; Samuni, A. *Free Radical Biol. Med.* **2002**, *32*, 872–881.
- (14) Akaike, T.; Yoshida, M.; Miyamoto, Y.; Sato, K.; Kohno, M.; Sasamoto, K.; Miyazaki, K.; Ueda, S.; Maeda, H. *Biochemistry* **1993**, *32*, 827–832.
- (15) Singh, R. J.; Hogg, N.; McHaourab, H. S.; Kalyanaraman, B. *Biochim. Biophys. Acta* **1994**, *1201*, 437–441.
- (16) Hogg, N.; Singh, R. J.; Joseph, J.; Neese, F.; Kalyanaraman, B. *Free Radical Res.* **1995**, *22*, 47–56.
- (17) Weber, H.; Grzesiok, A.; Sustmann, R.; Korth, H. G. *Z. Naturforsch., B: Chem. Sci.* **1994**, *49*, 1041–1050.
- (18) Damiani, E.; Greci, L.; Rizzoli, C. *J. Chem. Soc., Perkin Trans. 2* **2001**, 1139–1144.

of nitroxides toward $\cdot\text{NO}_2$, which is a key biological oxidant derived, for example, from decomposition of peroxyxynitrite in the absence and presence of CO_2 ,^{19,20} from peroxidase-catalyzed oxidation of nitrite,^{21–23} or from autoxidation of $\cdot\text{NO}$.^{24–26} The reaction of $\cdot\text{NO}_2$ with 4-OH-TPO and TPO to form the corresponding oxoammonium cations has been suggested to occur during the reduction of tetranitromethane by these nitroxides, and the rate constants were determined indirectly to be 1.2×10^5 and $2 \times 10^5 \text{ M}^{-1} \text{ s}^{-1}$, respectively.²⁷ Carroll et al.²⁸ proposed that during the decomposition of peroxyxynitrite the nitrosation of phenols takes place through the reaction of $\cdot\text{NO}_2$ with 4-OH-TPO, whereas Bonini et al.²⁹ assumed that this reaction does not take place because of the relatively low reduction potential of the $\cdot\text{NO}_2/\text{NO}_2^-$ couple (1.04 V³⁰). It was also assumed that $\cdot\text{NO}_2$ does not react with nitronyl nitroxides^{14–16} because a large excess of $\cdot\text{NO}_2$ had no effect on the EPR spectra and signal intensities of these nitroxides.¹⁴

In the present study, $\cdot\text{NO}_2$ was generated by pulse radiolysis, and its reaction with piperidine and pyrrolidine nitroxides was investigated. The nitroxides were found to react rapidly with $\cdot\text{NO}_2$ to form the respective oxoammonium cations, which can oxidize nitrite, ferrocyanide, or ABTS²⁻.

Experimental Section

Materials and Methods. All chemicals were of analytical grade and were used as received. Water for preparation of the solutions was distilled and purified using a Milli-Q purification system. The nitroxides TPO, 4-OH-TPO, and 3-carbamoylproxyl (3-CP) were purchased from Aldrich and 4-oxo-TPO, and its corresponding hydroxylamine, 4-oxo-TPO-H, were from Alexis Biochemicals. Fresh solutions of potassium ferrocyanide and 2,2'-azinobis(3-ethylbenzothiazoline-6-sulfonate) (ABTS²⁻) purchased from Sigma were prepared daily. Reduced β -nicotinamide adenine dinucleotide (NADH) grade III from yeast was obtained from Sigma. The concentration of NADH was determined spectrophotometrically using $\epsilon_{340} = 6200 \text{ M}^{-1} \text{ cm}^{-1}$. The hydroxylamines 4-OH-TPO-H and TPO-H were prepared by catalytic reduction using H_2 bubbled over Pt powder or by bubbling HCl gas through ethanolic solution of the nitroxide followed by drying. Fresh solutions of TPO-H and 4-OH-TPO-H were prepared immediately before each experiment to minimize oxidation to the nitroxide. The oxoammonium cations were prepared in aerated solutions containing 0.2 mM nitroxide in 4 mM phosphate buffer (PB) at pH 6.8 using an electrochemical reactor as previously described.³¹ The yield of TPO⁺ and 3-CP⁺ exceeded 94% as determined using ferrocyanide, which was immediately oxidized to ferricyanide ($\epsilon_{420} = 1000 \text{ M}^{-1} \text{ cm}^{-1}$). These oxoammonium cations were stable for at least 2 h. The final electrolyzed product in the case of 4-oxo-TPO did not oxidize ferrocyanide. Furthermore, the spectrum of the nitroxide was not restored upon

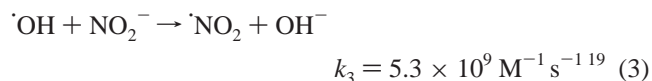
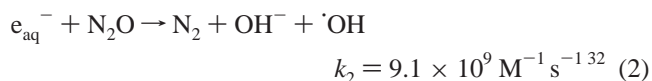
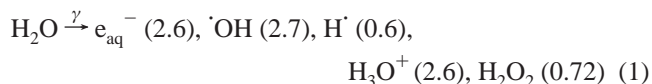
reversing the applied potential, suggesting that 4-oxo-TPO⁺ is rapidly converted into an unreactive species (see Discussion). Electrochemical oxidation of 4-OH-TPO yielded a mixture of 4-OH-TPO⁺ and the same end product as found during the electrooxidation of 4-oxo-TPO. The yield of 4-OH-TPO⁺ did not exceed 70%, and it was stable for only several minutes.

Electrooxidation of 1 mM 4-oxo-TPO in D_2O containing 4 mM K_2SO_4 was carried out for the ¹H NMR study. The oxidized nitroxides along with the respective hydroxylamines TPO-H and 4-oxo-TPO-H were scanned using a Mercury 300 NMR spectrometer of Varian Instruments. The proton parameters were obtained while suppressing the peak of water protons, and each of the samples was repeatedly pulsed at least 32 times. Product analysis was also carried out by HPLC-MS (LCQ ion trap equipped for electrospray, Finnigan Instrumentation).

Pulse radiolysis experiments were carried out using a 5-MeV Varian 7715 linear accelerator (0.05–1.5 μs electron pulses, 200 mA current). The dose per pulse was 2–29 Gy as determined with N_2O -saturated solutions containing 5 mM KSCN or ferrocyanide. A 200 W Xe lamp produced the analyzing light. Appropriate cutoff filters were used to minimize photochemistry. All measurements were made at room temperature by using a 4-cm spectroil cell and applying three light passes (optical path length 12.1 cm).

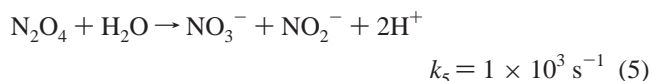
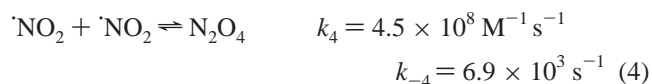
Results

Nitrogen dioxide was generated by irradiating N_2O -saturated ($\sim 25 \text{ mM}$) aqueous solutions containing 1–6 mM sodium nitrite and 4–8 mM phosphate (pH 6–8) or 1 mM acetate (pH 4.8) buffers through reactions 1–3 (in parentheses are the radiation-chemical yields of the species, which are defined as the number of species produced by 100 eV of absorbed energy. Yields are somewhat higher in the presence of high solute concentrations):



The yield of H^\cdot is ca. 10% of the total radical yield at pH > 3, and it adds rapidly to NO_2^- ($k = 1.6 \times 10^9 \text{ M}^{-1} \text{ s}^{-1}$) to form $\cdot\text{NO}$ in a process catalyzed by acids and bases.³³

The decay of $\cdot\text{NO}_2$ was followed at 400 nm ($\epsilon_{\text{max}} = 200 \text{ M}^{-1} \text{ cm}^{-1}$) and corresponded to the well-established pathway (reactions 4 and 5), where N_2O_4 hardly absorbs at this wavelength.³⁴



The half-life of $\cdot\text{NO}_2$ was not shortened by the addition of 500 μM TPO-H or 4-OH-TPO-H at pH 6.8. Because less than 20%

- (19) Merenyi, G.; Lind, J.; Goldstein, S.; Czapski, G. *J. Phys. Chem. A* **1999**, *103*, 5685–5691.
 (20) Goldstein, S.; Czapski, G. *J. Am. Chem. Soc.* **1998**, *120*, 3458–3463.
 (21) Byun, J.; Mueller, D. M.; Fabjan, J. S.; Heinecke, J. W. *Febs Lett.* **1999**, *455*, 243–246.
 (22) Reszka, K. J.; Matuszak, Z.; Chignell, C. F.; Dillon, J. *Free Radical Biol. Med.* **1999**, *26*, 669–678.
 (23) Burner, U.; Furtmuller, P. G.; Kettle, A. J.; Koppenol, W. H.; Obinger, C. *J. Biol. Chem.* **2000**, *275*, 20597–20601.
 (24) Ford, P. C.; Wink, D. A.; Stanbury, D. M. *Febs Lett.* **1993**, *326*, 1–3.
 (25) Lewis, R. S.; Tannenbaum, S. R.; Deen, W. M. *J. Am. Chem. Soc.* **1995**, *117*, 3933–3939.
 (26) Goldstein, S.; Czapski, G. *Inorg. Chem.* **1996**, *35*, 5935–5940.
 (27) Petrov, A. N.; Kozlov, Y. N. *Russ. J. Phys. Chem.* **1986**, *60*, 195–198.
 (28) Carroll, R. T.; Galatsis, P.; Borosky, S.; Kopec, K. K.; Kumar, V.; Althaus, J. S.; Hall, E. D. *Chem. Res. Toxicol.* **2000**, *13*, 294–300.
 (29) Bonini, M. G.; Mason, R. P.; Augusto, O. *Chem. Res. Toxicol.* **2002**, *15*, 506–511.
 (30) Stanbury, D. M. *Adv. Inorg. Chem.* **1989**, *33*, 69–138.
 (31) Goldstein, S.; Merenyi, G.; Russo, A.; Samuni, A. *J. Am. Chem. Soc.* **2003**, *125*, 789–795.

- (32) Mallard, W. G.; Ross, A. B.; Helman, W. P. *NIST Standard References Database 40, Version 3.0*, 1998.
 (33) Lyman, S. V.; Schwarz, H. A.; Czapski, G. *J. Phys. Chem. A* **2002**, *106*, 7245–7250.
 (34) Gratzel, M.; Henglein, A.; Lilie, J.; Beck, G. *Ber. Bunsen-Ges. Phys. Chem.* **1969**, *73*, 646.

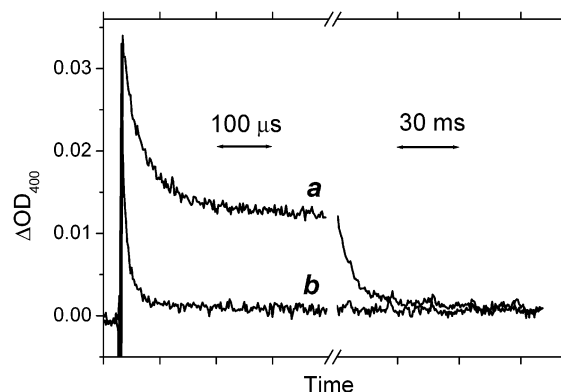


Figure 1. The decay of $\cdot\text{NO}_2$ with and without 4-OH-TPO. The decay of $\cdot\text{NO}_2$ was followed at 400 nm upon pulse-irradiation (29 Gy/pulse) of N_2O -saturated solutions containing 2 mM nitrite and 4 mM PB at pH 6.8 in the absence (a) and in the presence of 150 μM 4-OH-TPO (b). The optical path length was 12.1 cm.

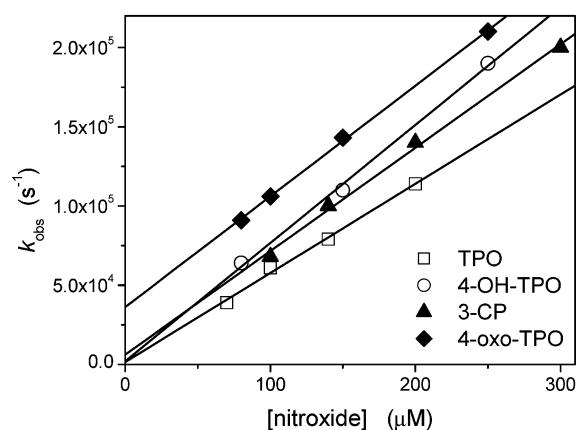


Figure 2. The observed rate constant of the decay of $\cdot\text{NO}_2$ as a function of [nitroxide]. All solutions were N_2O -saturated and contained 2 mM NO_2^- and 4 mM PB at pH 6.8. The dose was 12–29 Gy/pulse.

acceleration of $\cdot\text{NO}_2$ decay would be readily detectable, the upper limit for the rate constant of the reaction of $\cdot\text{NO}_2$ with these hydroxylamines can be estimated to be $1 \times 10^5 \text{ M}^{-1} \text{ s}^{-1}$.

The establishment of equilibrium 4 is a relatively fast second-order process, which upon the addition of 80–300 μM nitroxide turned into a fast first-order reaction as a result of reaction 6.



Typical kinetic traces for the decay of ca. 16 μM $\cdot\text{NO}_2$ alone and in the presence of 150 μM 4-OH-TPO are shown in Figure 1.

The decay of $\cdot\text{NO}_2$ in the presence of TPO and 4-OH-TPO was first-order, and k_{obs} was linearly dependent on [nitroxide]₀ (Figure 2) and independent of the pH over the range 3.9–10.2. In the presence of 4-oxo-TPO and 3-CP, the fast first-order decay of $\cdot\text{NO}_2$ was followed by a slower second-order decay. The observed first-order rate constant was linearly dependent on [nitroxide]₀ (Figure 2), whereas the rate of the slow second-order decay increased upon decreasing [nitroxide]₀ and increasing $[\text{NO}_2^-]$. The rate constant of reaction 6 was calculated from the slopes of the lines in Figure 2, and the results are summarized in Table 1.

In the presence of each of the four nitroxides tested, the formation and decay of $\cdot\text{NO}_2$, which were followed at 400 nm,

were accompanied by the appearance of a transient observed in the UV region. Typical kinetic traces at 290 and 400 nm are shown in Figure 3 for 3-CP, where $\Delta\epsilon_{290} = 670 \pm 50 \text{ M}^{-1} \text{ cm}^{-1}$.

In the case of TPO, the decay of the transient absorption at 290 nm was too slow to study by our setup. In the case of the other nitroxides, the decay of the absorption exhibited second-order kinetics, and k_{obs} was linearly dependent on $[\text{nitroxide}]_0^{-2}$ at a constant $[\text{NO}_2^-]_0$ and on $[\text{NO}_2^-]_0^2$ at a constant [nitroxide]₀ (Figures 4 and 5).

The decay of $\cdot\text{NO}_2$ was unaffected by the number of pulses delivered into the solution, which suggests that there is no loss of the nitroxides during this process. After repetitive pulsing (340 Gy) of N_2O -saturated solution containing 200 μM nitroxide and 2 mM nitrite at pH 6.8, the solution was transferred to a diode array spectrophotometer, and the spectrum was recorded within less than 1 min after the irradiation. No appreciable spectral changes were observed for 4-OH-TPO, 4-oxo-TPO, and 3-CP. In the case of TPO, the product of the irradiated sample was identified as TPO^+ , which decayed slowly with a first half-life of about 30 min in the presence of 2 mM nitrite.

Reaction of $\cdot\text{NO}_2$ with Nitroxide in the Presence of ABTS^{2-} or Ferrocyanide. The rate constants for the reaction of $\cdot\text{NO}_2$ with ABTS^{2-} and ferrocyanide have been previously determined to be 2.2×10^7 and $3 \times 10^6 \text{ M}^{-1} \text{ s}^{-1}$, respectively.³² The $\cdot\text{NO}_2$ -induced formation of $\text{ABTS}^{\cdot-}$ ($\epsilon_{660} = 12\,000 \text{ M}^{-1} \text{ cm}^{-1}$) or ferricyanide ($\epsilon_{420} = 1000 \text{ M}^{-1} \text{ cm}^{-1}$) was followed in the absence and presence of various concentrations of the nitroxide upon pulse-irradiation of N_2O -saturated solutions containing 4 mM nitrite at pH 6.8 ($[\cdot\text{NO}_2]_0 = 1.4\text{--}4 \mu\text{M}$). The yields of $\text{ABTS}^{\cdot-}$ or ferricyanide were unaffected upon the addition of the various nitroxides, whereas the formation rate increased linearly with the increase in the concentration of the nitroxide. The observed first-order rate constant of the formation of $\text{ABTS}^{\cdot-}$ as a function of [nitroxide]₀ is given in Figure 6 (only a few data points obtained in the presence of $\text{Fe}(\text{CN})_6^{4-}$ were included to avoid overloading the figure).

The formation rate was almost unaffected by $[\text{ABTS}^{2-}]_0$ or $[\text{Fe}(\text{CN})_6^{4-}]_0$, for example, less than 10% increase in k_{obs} when $[\text{ABTS}^{2-}]_0$ was increased from 100 to 500 μM in the presence of 100 μM nitroxide. The results indicate that $\cdot\text{NO}_2$ reacts with the nitroxide to form a reactive intermediate, which oxidizes ABTS^{2-} or $\text{Fe}(\text{CN})_6^{4-}$ with a diffusion-controlled rate constant. Hence, the rate-determining step is the reaction of $\cdot\text{NO}_2$ with the nitroxide (reaction 6), and the rates of formation of $\text{ABTS}^{\cdot-}$ and ferricyanide in the presence of all nitroxides tested are the same (Figure 6), both being characterized by k_6 . From the slope of the lines in Figure 6, we calculated k_6 (Table 1).

The Case of 4-oxo-TPO. In contrast to TPO, 4-OH-TPO, and 3-CP, the electrochemical oxidation of 4-oxo-TPO forms a relatively unreactive product, which does not oxidize ABTS^{2-} or ferrocyanide. We have recently shown that TPO^+ and 3-CP^+ react with NADH via a two-electron-transfer mechanism to form the corresponding hydroxylamine and NAD^+ .³¹ In contrast, the product accumulated during electrooxidation of 4-oxo-TPO was stable for at least 3 h in the presence of NADH at pH 6.8. However, about 4 μM NADH was consumed when 4 μM $\cdot\text{NO}_2$ reacted with 50 or 100 μM 4-oxo-TPO in the presence of 100 μM NADH and 4 mM nitrite at pH 6.8. The decay of NADH

Table 1. Summary of All Rate Constants and Reduction Potentials Determined in the Present Study

	TPO	4-OH-TPO	4-oxo-TPO	3-CP
k_6 , $M^{-1} s^{-1}$ (Figure 2, direct)	$(5.6 \pm 0.3) \times 10^8$	$(7.5 \pm 0.4) \times 10^8$	$(6.3 \pm 0.2) \times 10^8$	$(6.5 \pm 0.3) \times 10^8$
k_6 , $M^{-1} s^{-1}$ (Figure 6, ABTS ²⁻)	$(7.1 \pm 0.2) \times 10^8$	$(8.7 \pm 0.2) \times 10^8$	$(7.1 \pm 0.2) \times 10^8$	$(7.1 \pm 0.2) \times 10^8$
k_6 , $M^{-1} s^{-1}$ (Figure 6, Fe(CN) ₆ ⁴⁻) ^a	$(6.7 \pm 0.2) \times 10^8$	$(7.8 \pm 0.2) \times 10^8$	$(6.7 \pm 0.3) \times 10^8$	$(6.7 \pm 0.3) \times 10^8$
K_6	$(8 \pm 4) \times 10^4$ ^b	$(2.9 \pm 0.2) \times 10^3$	63 ± 7	450 ± 20
k_{-6} , $M^{-1} s^{-1}$	$(9 \pm 4) \times 10^3$	$(2.7 \pm 0.4) \times 10^5$	$(1.1 \pm 0.2) \times 10^7$	$(1.5 \pm 0.2) \times 10^6$
$E^\circ(\text{RN}^+=\text{O}/\text{RNO}^-)$, V	0.75 ³¹	0.84	0.93	0.88
k_6 , $M^{-1} s^{-1}$ (Marcus equation)	5×10^7 ^c	1×10^7 ^c	2×10^6 ^c	6×10^6 ^c
k_9 , $M^{-1} s^{-1}$	4×10^6 ^d	9×10^5 ^d	2×10^5 ^d	4×10^5 ^d
	ND ^e	ND	$(7 \pm 1) \times 10^8$	ND

^a The rate constant was calculated from the slopes of the lines as seen in Figure 6, although not all of the data points were included. The results in the presence of Fe(CN)₆⁴⁻ are within experimental error identical to those determined in the presence of ABTS²⁻. We included in Figure 6 only a few data points for each nitroxide to avoid overloading the figure. ^b Calculated using k_7 and $E^\circ(\text{TPO}^+/\text{TPO}) = 0.75 \pm 0.01$ V.³¹ ^c Assuming that the self-exchange rate constant for RNO⁻/RN⁺ is $1 \times 10^{10} M^{-1} s^{-1}$. ^d Assuming that the self-exchange rate constant for RNO⁻/RN⁺ is $5 \times 10^7 M^{-1} s^{-1}$.⁴² ^e ND – not determined.

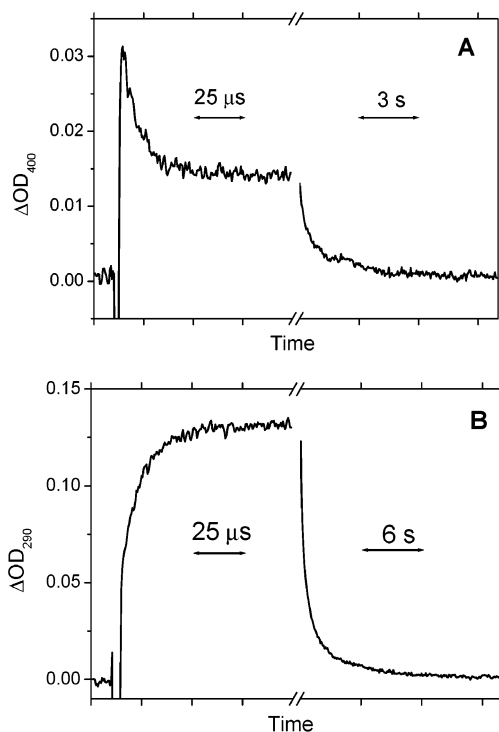


Figure 3. The reaction of 3-CP with $\cdot\text{NO}_2$. The formation and decay of $\cdot\text{NO}_2$ were followed at 400 nm (A), whereas those of the transient formed during this reaction were monitored at 290 nm (B). N_2O -saturated solutions containing $140 \mu\text{M}$ 3-CP and 2 mM nitrite at pH 6.8 (4 mM PB) were pulse-irradiated (29 Gy/pulse). The optical path length was 12.1 cm.

at 385 nm ($\epsilon = 830 M^{-1} \text{cm}^{-1}$) was first-order with $k_{\text{obs}} = (1.4 \pm 0.1) \times 10^4$ or $(2.3 \pm 0.1) \times 10^4 s^{-1}$, respectively. These results show that the reaction of $\cdot\text{NO}_2$ with 4-oxo-TPO forms a reactive intermediate, which oxidizes NADH, and that the former reaction is not rate-limiting as in the case of ferrocyanide or ABTS²⁻.

We have previously shown that TPO and 3-CP were almost fully recovered (ca. 94%) when their electrooxidized solution was subjected to electroreduction.³¹ Conversely, the spectrum of 4-oxo-TPO was not recovered upon reduction, and the spectrum of the reduced product was hardly affected upon subsequent electrooxidation. We therefore conclude that the electrooxidation of 4-oxo-TPO forms an unstable oxoammonium

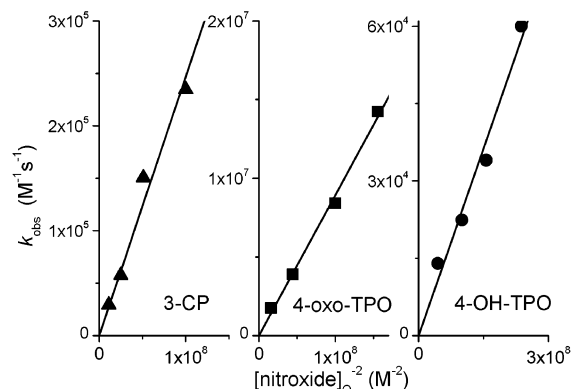


Figure 4. The effect of nitroxide concentrations on the decay rate of the transient absorption at 290 nm. The effect of [3-CP]₀ and [4-oxo-TPO]₀ in the presence of 2 mM nitrite and that of [4-OH-TPO]₀ in the presence of 4 mM nitrite were studied. All solutions were N_2O -saturated and contained 4 mM PB at pH 6.8. The dose was 29 Gy/pulse.

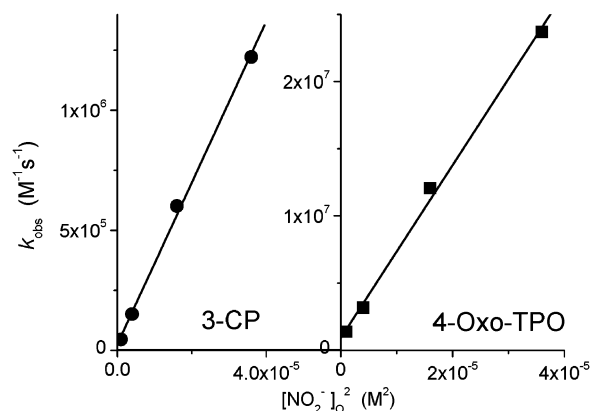


Figure 5. The effect of nitrite concentrations on the decay rate of the transient absorption at 290 nm. The effect of $[\text{NO}_2^-]_0$ in the presence of $140 \mu\text{M}$ 3-CP or $150 \mu\text{M}$ 4-oxo-TPO was studied. All solutions were N_2O -saturated and contained 4 mM PB at pH 6.8. The dose was 29 Gy/pulse.

cation, which decays during the electrolysis process into a relatively unreactive species. We used HPLC-MS to compare the spectra of 4-oxo-TPO with that of its electrooxidation product. We failed to detect the anticipated peak of 170+1 due to 4-oxo-TPO itself, presumably because of a poor pickup of a proton by the parent nitroxide. However, for the electrooxidized product, we observed a peak of 170 that could not be attributed

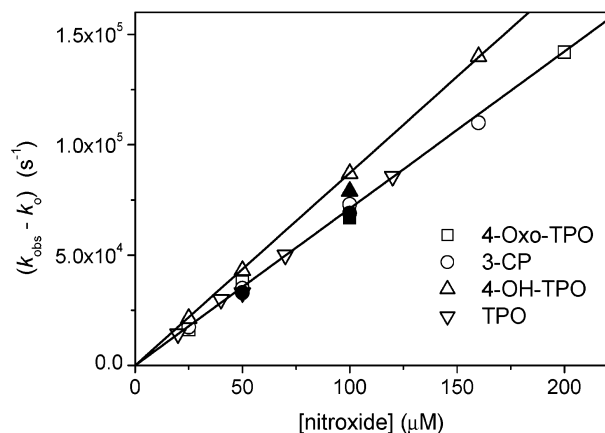
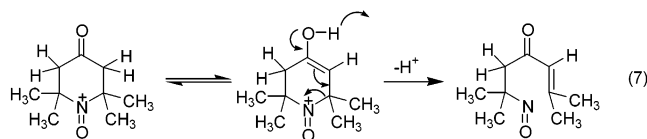


Figure 6. The observed rate constant for the formation of $\text{ABTS}^{\cdot-}$ (open symbols) or $\text{Fe}(\text{CN})_6^{3-}$ (solid symbols) as a function of nitroxide concentration. All solutions were N_2O -saturated and contained 4 mM NO_2^- , 250–500 μM ABTS^{2-} or $\text{Fe}(\text{CN})_6^{4-}$, and 8 mM PB at pH 6.8. The dose was 2.4 or 6.9 Gy/pulse, and k_0 is the observed rate of the formation of $\text{ABTS}^{\cdot-}$ or $\text{Fe}(\text{CN})_6^{3-}$ in the absence of nitroxide, that is, $k_0 = 2 \times 10^7$ [ABTS^{2-}] or 3×10^6 [$\text{Fe}(\text{CN})_6^{4-}$]. The results in the presence of $\text{Fe}(\text{CN})_6^{4-}$ are within experimental error identical to those obtained in the presence of ABTS^{2-} . We included only a few data points for each nitroxide to avoid overloading the figure.

to 4-oxo-TPO⁺, which is already charged, but to a novel uncharged species having a MW of 169. We therefore suggest that 4-oxo-TPO⁺ undergoes a rapid β -elimination of proton via eq 7:



To verify our suggestion, we electrooxidized 4-oxo-TPO in D_2O and compared the ^1H NMR spectrum of the product to that of 4-oxo-TPO-H. The spectrum of the hydroxylamine (Figure 7, bottom), which consisted of a singlet at 1.48 ppm due to 12 protons of the methyls at the 2 and 6 positions, and a singlet at 2.87 ppm corresponding to the 4 protons at the 3 and 5 positions, was anticipated to resemble that of 4-oxo-TPO⁺. In fact, it greatly differed from that observed for the electrooxidation product (Figure 7, top). The latter showed a singlet at 1.55 ppm due to protons of the 2 methyls bound to the carbon with the nitroso group (position 1), a singlet at 2.2 ppm attributable to the protons of the methyls at position 5, and a singlet at 2.99 ppm due to the 2 protons at position 2. The expected singlet of the vinylic proton was overshadowed by the large water peak at 4.8 ppm, which was present in all of our samples.

Generally, aliphatic C-nitroso compounds can exist as monomers, colorless dimers, or tautomeric oximes. However, tertiary nitroso compounds often exist as monomers, which are colored and exhibit a typical absorption band between 630 and 790 nm ($\epsilon = 1\text{--}60 \text{ M}^{-1} \text{ cm}^{-1}$).³⁵ This further supports our conclusion because the electrooxidized product absorbs at 650 nm ($\epsilon = \text{ca. } 14 \text{ M}^{-1} \text{ cm}^{-1}$).³⁶

(35) Williams, D. L. H. *Nitrosation*; Cambridge University Press: Cambridge, 1988.

(36) Samuni, A.; Goldstein, S.; Russo, A.; Mitchell, J. B.; Krishna, M. C.; Neta, P. *J. Am. Chem. Soc.* **2002**, *124*, 8719–8724.

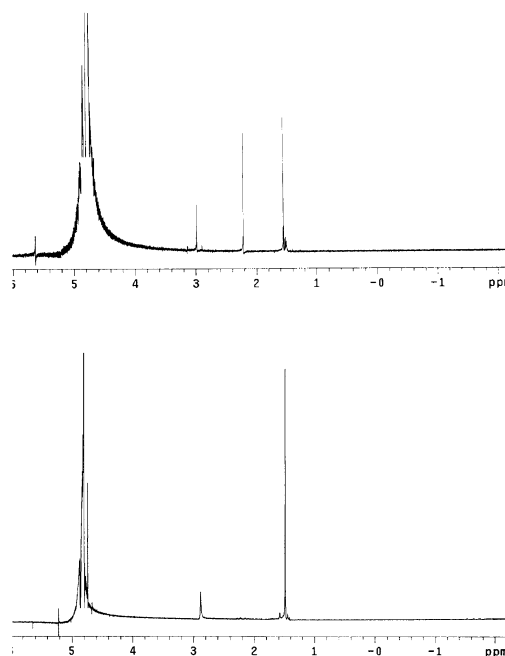
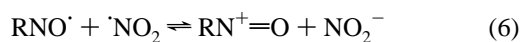


Figure 7. The ^1H NMR spectrum of 4-oxo-TPO-H (bottom) and the electrooxidation product of 4-oxo-TPO (top) in D_2O (structure given in eq 7). The spectrum of the hydroxylamine consisted of a singlet at 1.48 ppm (12 protons of the methyls at the 2 and 6 positions) and a singlet at 2.87 ppm (4 protons at the 3 and 5 positions). The spectrum of the electrooxidation product showed a singlet at 1.55 ppm (6 protons of the methyls at position 1), a singlet at 2.2 ppm (6 protons of the methyls at position 5), and a singlet at 2.99 ppm (2 protons at position 2).

We have previously found that the reaction of $\cdot\text{OH}$ or $\cdot\text{N}_3$ with 4-oxo-TPO forms the same species as that produced electrochemically, but with different yields.³⁶ We have mistakenly identified this product as 4-oxo-TPO⁺, on the basis of the observation that, after partial oxidation of 3.66 mM 4-oxo-TPO, the spectrum of the nitroxide in the visible region was almost fully recovered upon subsequent electroreduction. However, a closer examination of the UV and visible spectrum after complete oxidation at low and high concentrations of the nitroxide suggests that the nitroxide was not restored when the electrooxidized solution was subjected to electroreduction. Thus, the reaction of 4-oxo-TPO with $\cdot\text{OH}$ or $\cdot\text{N}_3$ forms the unstable 4-oxo-TPO⁺, which decays in the absence of a potential reductant into the same species as is formed electrochemically.

Discussion

The reaction of $\cdot\text{NO}_2$ with nitroxides forms an intermediate which can oxidize ferrocyanide, ABTS^{2-} , NADH, and nitrite. In the case of TPO, the intermediate reacted sufficiently slowly with nitrite for it to be identified spectrophotometrically as TPO⁺. In the case of the other nitroxides, the intermediates decayed faster in the presence of nitrite via a second-order reaction. The observed second-order rate constant was linearly dependent on $[\text{nitroxide}]_0^{-2}$ at a constant $[\text{NO}_2^-]_0$, and on $[\text{NO}_2^-]_0^2$ at a constant $[\text{nitroxide}]_0$ (Figures 4, 5). These results suggest that the respective oxoammonium cations are formed via reaction 6 and decomposed slowly via reaction -6 followed by reactions 4 and 5.

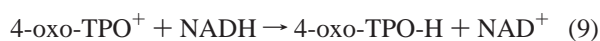


Assuming that reaction 6 is a fast approach to equilibrium, we found that the rate-limiting step for the decay of $\text{RN}^+=\text{O}$ is the dimerization/hydrolysis of $\cdot\text{NO}_2$, and rate eq 8 is obtained,

$$-\frac{d[\text{RN}^+=\text{O}]}{dt} = \frac{2k_4k_5[\text{NO}_2^-]_0^2[\text{RN}^+=\text{O}]^2}{(k_{-4} + k_5)K_6^2[\text{RNO}\cdot]_0^2} = k_{\text{obs}}[\text{RN}^+=\text{O}]^2 \quad (8)$$

where from the literature $2k_4k_5/(k_{-4} + k_5) = 1.3 \times 10^8 \text{ M}^{-1} \text{ s}^{-1}$ is calculated. Hence, $k_{\text{obs}} = 1.3 \times 10^8([\text{NO}_2^-]_0/K_6[\text{RNO}\cdot]_0)^2$, and plots of k_{obs} versus $1/[\text{RNO}\cdot]_0^2$ or $[\text{NO}_2^-]_0^2$ should be linear (Figures 4 and 5) with slope1 = $1.3 \times 10^8([\text{NO}_2^-]_0/K_6)^2$ or slope2 = $1.3 \times 10^8/([\text{RNO}\cdot]_0/K_6)^2$, respectively, and (slope1/slope2)^{1/2} = $[\text{RNO}\cdot]_0/[\text{NO}_2^-]_0$. Hence, (slope1/slope2)^{1/2} = $(2.6 \pm 0.1) \times 10^{-7}$ and $(3.7 \pm 0.1) \times 10^{-7} \text{ M}^2$ for 3-CP and 4-oxo-TPO, respectively, and are in good agreement with the experimental conditions, that is, 2 mM nitrite and 140 μM 3-CP or 150 μM 4-oxo-TPO. The values of K_6 , which are derived from the slope of the lines in Figures 4 and 5, are summarized in Table 1.

The rate constant for the oxidation of ferrocyanide and ABTS^{2-} by $\text{RN}^+=\text{O}$ is extremely high, that is, ca. $1 \times 10^{10} \text{ M}^{-1} \text{ s}^{-1}$, which explains why the rate-determining step of the formation of the oxidized product is the reaction of $\cdot\text{NO}_2$ with the nitroxide. We simulated the formation of NAD^+ using reactions 4–6 and 9 for the reaction of 4 μM $\cdot\text{NO}_2$ with 50 or 100 μM 4-oxo-TPO in the presence of 100 μM NADH and 4 mM nitrite, where $k_{\text{obs}} = (1.4 \pm 0.1) \times 10^4$ or $(2.3 \pm 0.1) \times 10^4 \text{ s}^{-1}$, respectively, and obtained $k_9 = (7 \pm 1) \times 10^8 \text{ M}^{-1} \text{ s}^{-1}$.



The reduction potentials of the $\text{RN}^+=\text{O}/\text{RNO}\cdot$ couples have been calculated using K_6 and $E^\circ(\text{NO}_2/\text{NO}_2^-) = 1.04 \text{ V}$ to be 0.84, 0.93, and 0.88 V for 4-OH-TPO, 4-oxo-TPO, and 3-CP, respectively. The latter value is in excellent agreement with that determined previously using $\text{HO}_2\cdot$ as an oxidant, that is, 0.89 V.³¹ The calculated reduction potentials for all nitroxides are in good agreement with the midpotentials, which have been previously determined by cyclic voltammetry.^{37–39} In the case of TPO, we calculated $K_6 = 8 \times 10^4$ using the recent value of 0.75 V for $E^\circ(\text{TPO}^+/\text{TPO})$.³¹ The results are compiled in Table 1.

As in the case of $\text{HO}_2\cdot$,³¹ one can use the Marcus equation $k_6 = (k_a k_b K_6 f)^{1/2}$ (k_a and k_b are the self-exchange rate constants for the reactants, $\ln f = (\ln K_6)^2/4 \ln(k_a k_b/10^{22})$)⁴⁰ to show that reaction 6 does not take place via an outer-sphere electron-transfer mechanism. The self-exchange rate constant for $\text{NO}_2/\text{NO}_2^-$ has been determined to be $9.6 \text{ M}^{-1} \text{ s}^{-1}$.⁴¹ The self-exchange rate constant for X-TPO/X-TPO⁺ in acetonitrile has been determined by EPR and ¹H NMR to be 5.7×10^7 and 4.4

$\times 10^7 \text{ M}^{-1} \text{ s}^{-1}$ for X = OCH_3 and OCOCH_3 , respectively.⁴² In acetonitrile, the rates are expected to be similar for nitroxides studied by us. If anything, these rates should be smaller in water, because in the latter solvent a stronger solvation of the cation should increase the outer-sphere components of the barrier to the electron self-exchange. Still, $1 \times 10^{10} \text{ M}^{-1} \text{ s}^{-1}$ must surely be considered a generous upper limit. As seen in Table 1, the calculated values for k_6 are at least 1–2 orders of magnitude lower than the experimental values (Table 1). Therefore, reaction 6 most probably takes place via an inner-sphere electron-transfer mechanism,



where $k_6 = k_{10}k_{11}/(k_{-10} + k_{11})$.

Petrov and Kozlov²⁷ studied the reaction of nitroxides with tetranitromethane in the presence of nitrite and measured the concentrations of the reagents and products at the minimum concentration of the nitroxide under different initial concentrations of the reagents. A complex linear relationship yielded a straight line, and from the slopes of the lines they determined $K_6 = 2.7 \times 10^3$ and 7×10^4 for 4-OH-TPO and TPO, which are in excellent agreement with our determination. However, from the intercepts of these lines, they derived $k_6 = 1.2 \times 10^5$ and $2 \times 10^5 \text{ M}^{-1} \text{ s}^{-1}$ for 4-OH-TPO and TPO, respectively, which are more than 3 orders of magnitude lower than those determined directly (Table 1). Most likely, their approach was not sensitive enough for accurate determination of k_6 .

The present study may explain why a large excess of $\cdot\text{NO}_2$ had no effect on the EPR spectra and signal intensities of nitronyl nitroxides.¹⁴ These nitroxides are expected to react rapidly with $\cdot\text{NO}_2$ to form the corresponding nitronyl oxoammonium cations, which could be reduced back to the nitroxides in the presence of nitrite formed mainly via the self-decomposition of the large excess of $\cdot\text{NO}_2$ in aqueous solutions (reactions 4–5).

Conclusions

The rate constants determined in the present study for the reaction of $\cdot\text{NO}_2$ with piperidine and pyrrolidine nitroxides were determined to be $(7\text{--}8) \times 10^8 \text{ M}^{-1} \text{ s}^{-1}$ and are close to that determined for the reaction of $\cdot\text{NO}$ with $\cdot\text{NO}_2$, that is, $1.1 \times 10^9 \text{ M}^{-1} \text{ s}^{-1}$.⁴³ These are among the highest rate constants measured for $\cdot\text{NO}_2$ at physiological pH⁴⁴ and exceed by far those with glutathione, cysteine, and urate, which are considered to be the major scavengers of the radical in biological systems.⁴⁵ The kinetics results demonstrate that the reaction proceeds via an inner-sphere electron-transfer mechanism to form the respective oxoammonium cation, which is reduced back to the nitroxide while oxidizing nitrite to $\cdot\text{NO}_2$. Hence, the nitroxide slows down the decomposition of $\cdot\text{NO}_2$ into nitrite

(37) Fish, J. R.; Swarts, S. G.; Sevilla, M. D.; Malinski, T. J. *Phys. Chem.* **1988**, *92*, 3745–3751.

(38) Morris, S.; Sosnovsky, G.; Hui, B.; Huber, C. O.; Rao, N. U. M.; Swartz, H. M. *J. Pharm. Sci.* **1991**, *80*, 149–152.

(39) Krishna, M. C.; Grahame, D. A.; Samuni, A.; Mitchell, J. B.; Russo, A. *Proc. Natl. Acad. Sci. U.S.A.* **1992**, *89*, 5537–5541.

(40) Marcus, R. A. *J. Phys. Chem.* **1963**, *67*, 853–857.

(41) Awad, H. H.; Stanbury, D. M. *J. Am. Chem. Soc.* **1993**, *115*, 3636–3642.

(42) Wu, L. M.; Guo, X.; Wang, J.; Guo, Q. X.; Liu, Z. L.; Liu, Y. C. *Sci. China, Ser. B* **1999**, *42*, 138–144.

(43) Gratzel, M.; Taniguchi, S.; Henglein, A. *Ber. Bunsen-Ges. Phys. Chem.* **1970**, *74*, 488–492.

(44) Huie, R. E. *Toxicology* **1994**, *89*, 193–216.

(45) Ford, E.; Hughes, M. N.; Wardman, P. *Free Radical Biol. Med.* **2002**, *32*, 1314–1323.

and nitrate and could serve as a reservoir of $\cdot\text{NO}_2$ radicals. Moreover, the respective oxoammonium cation could oxidize biological targets, causing further damage unless it is reduced back to the nitroxide by common biological reductants, such as thiols or urate. These subsequent processes are currently under investigation.

Acknowledgment. This research was supported (A.S.) by a grant from the Israel Science Foundation of the Israel Academy of Sciences. We thank Dr. Henry Fales for mass spectroscopic analysis and Dr. Gabor Merenyi for helpful discussions.

JA035286X